

# OPTIMIZING THE BEAM-BEAM ALIGNMENT IN AN ELECTRON LENS USING BREMSSTRAHLUNG

C. Montag, W. Fischer, D. Gassner, P. Thieberger, BNL, Upton, NY 11973, USA  
E. Haug, University of Tübingen, Germany

## Abstract

Installation of electron lenses for the purpose of head-on beam-beam compensation is foreseen at RHIC. To optimize the relative alignment of the electron lens beam with the circulating proton (or ion) beam, photon detectors will be installed to measure the bremsstrahlung generated by momentum transfer from protons to electrons. We present the detector layout and simulations of the bremsstrahlung signal as function of beam offset and crossing angle.

## INTRODUCTION

Luminosity performance of the Relativistic Heavy Ion Collider (RHIC) in proton operations is limited by the beam-beam effect. To overcome this limitation, installation of electron lenses is foreseen in the two RHIC rings, thus providing head-on beam-beam compensation [1]. Each of these lenses provides an intense electron beam, the transverse Gaussian distribution of which matches the profile of the oncoming proton beam. When this electron beam is brought into head-on collisions with the circulating proton beam, it provides a beam-beam kick of equal magnitude but opposite sign to that from the oncoming proton beam. If the betatron phase advance between the proton-proton interaction point (IP) and the electron lens equals an integer multiple of 180 degrees, the nonlinear beam-beam kick at the IP is therefore completely compensated by the opposite kick at the electron lens, provided that the beam transport between these two locations is linear.

In reality, the beam transport between the IP and the electron lens is non-linear due to the presence of chromaticity correction sextupoles. The electron lens therefore needs to be installed as close as possible to the IP to keep the nonlinearities in the beamline at a minimum. Furthermore, providing the ideal phase advance between each of the IPs and the electron lens is extremely challenging. Thus, head-on beam-beam compensation of only one of the two RHIC interaction points is planned.

The interaction of the high energy proton beam with the electron lens results in the emission of bremsstrahlung due to the momentum transfer from the protons to the low energy electrons [2]. This radiation can be used as a luminosity signal to align the orbits of the electron and proton beams. Because of the non-relativistic electron beam energy, the spatial distribution of the emitted photons is almost isotropic, as schematically illustrated in Figure 1. The blue lines within the circles are the photon trajectories in the proton rest frame for two cases. The left column

shows isotropic emission and the one to the right shows cones of photons qualitatively similar to bremsstrahlung radiation produced by electrons impinging from the right. The opening angle of these cones is proportional to  $1/\gamma$ . The red lines indicate the calculated angles that would be observed in the electron rest frame. We see that for the uniform emission, most of the rays are swept forward for large values of  $\gamma$  (the so called “headlight effect”) except the very few ones that are closest to being emitted in the backward direction. For the bremsstrahlung case, most of the rays are close to that direction and are therefore not totally swept forward. The higher the  $\gamma$ , the stronger the “headlight effect”, but correspondingly the bremsstrahlung cone gets narrower and the two effects essentially cancel. This is also what happens in our case. The angular distribution of photons from fast protons on slow electrons is not narrow. However, the results cannot be compared in detail because here we do not use a real bremsstrahlung distribution in the proton rest frame; just cones with representative widths.

A different way of tackling this problem is presented by Jackson [3], arguing that the problem is essentially non-relativistic. The almost stationary electrons get accelerated by the field of the passing proton, and emit photons due to that acceleration. The fact that the proton is highly relativistic does not really matter much. Its only role is to accelerate the electron, which never becomes very relativistic. The only way the  $\gamma$  of the proton enters is in affecting the shape of the field (mostly perpendicular) seen by the electron. A wide angular distribution also results with this approach.

Figure 2 shows the differential cross section  $d^2\sigma/(dk \cdot d\Omega_k)$ , for  $E_p = 250$  GeV,  $E_e = 10$  keV, and a photon energy of  $k = 10$  keV as an example.

## DETECTOR ARRANGEMENT

Taking advantage of this “light bulb” characteristics, two photon detectors will be installed near the ends of the electron lens, as schematically depicted in Figure 3. This configuration allows us to maximize the overlap of the proton and electron beam by eliminating relative offsets and crossing angles.

In the following, we assume a  $l = 2$  m long electron lens with a beam pipe radius  $r = 4$  cm. Two  $2 \times 2$  cm<sup>2</sup> photon detectors are located in the beam pipe wall at both ends of the lens. Beam sizes and intensities are listed in Table 1. In the case of a parallel offset  $\Delta r$  of the two beams with respect to each other, the luminosity and therefore the

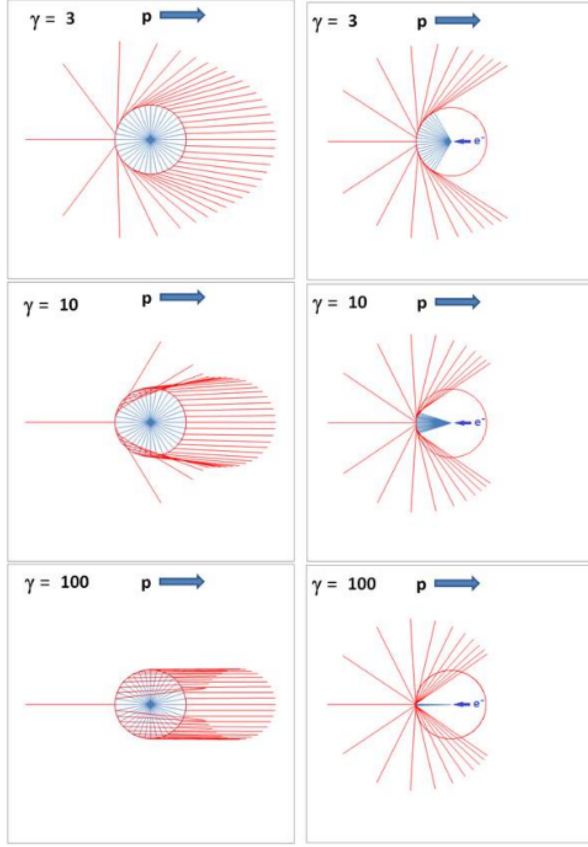


Figure 1: Trajectories of photons emitted in the proton rest frame (blue) and corresponding angles in the electron rest frame (red). Cases are shown for relativistic  $\gamma$  values increasing from top to bottom and for isotropic emission (left) and emission within a cone with opening angle proportional to  $1/\gamma$  (right). The same relativistic angle transformation (the so called relativistic aberration) is applied both at left and at right.

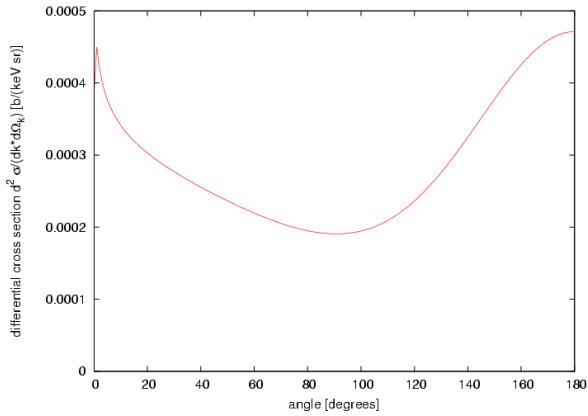


Figure 2: Differential cross section  $d^2\sigma/(dk \cdot d\Omega_k)$ , calculated in the lab frame for  $E_p = 250$  GeV,  $E_e = 10$  keV, and a photon energy of  $k = 10$  keV. Zero degrees corresponds to the direction of the proton beam.

Table 1: RHIC electron lens parameters. Case 1 refers to the electron lens upgrade for 250 GeV proton beam energy. Case 2 is also for 250 GeV, but with a proton bunch intensity increased by 50%.

parameter	unit	case 1	case 2
<b>proton beam</b>			
beam energy $E_p$	GeV	250	250
relativistic $\gamma_p$		266	266
bunch intensity $N_p$	$10^{11}$	2.0	3.0
no of colliding bunches		107	107
average beam current	mA	270	405
transverse rms emittance $\epsilon_n$	mm mrad	2.5	2.5
$\beta_{x,y}$ at e-lens location	m	10	10
$\beta_{x,y}$ at IP6, IP8	m	0.5	0.5
rms beam size at e-lens location	$\mu\text{m}$	310	310
rms beam size at IP6, IP8	$\mu\text{m}$	70	70
no of beam-beam IPs	...	2	2
beam-beam compensation degree	%	50	50
<b>main solenoid section</b>			
beam pipe radius $R$	mm	— 40.0 —	
electron rms beam size $\sigma_e$	$\mu\text{m}$	310	310
solenoid length	m	— 2.5 —	
length of good field quality $L$	m	— 2.1 —	
solenoid field strength $B_{sm}$	T	— 6.0 —	
no of electrons seen by protons	$10^{11}$	2.0	3.0
no of electrons in lens	$10^{11}$	1.7	2.5
integrated current $(I_e L)$	A m	1.3	2.3

photon yield scales as

$$L = L_0 \cdot \exp\left(-\frac{(\Delta r)^2}{2\sigma^2}\right), \quad (1)$$

while for a crossing angle  $\Delta\phi$  the luminosity contribution from each infinitesimal slice of thickness  $ds$  depends on its longitudinal position  $s$  within the electron lens. With  $s_0 = 0$  being the center of the electron lens, the luminosity contribution from each slice at position  $s$  is therefore

$$dL(s) = dL_0(s) \cdot \exp\left(-\frac{(\Delta r(s))^2}{2\sigma^2}\right), \quad (2)$$

with

$$\Delta r(s) = \phi \cdot s. \quad (3)$$

Using the detector arrangement depicted in Figure 3, we can therefore calculate the photon yield in the two detectors as a function of the parallel beam offset  $\Delta r$  and the crossing angle  $\phi$ , as shown in Figures 4 and 5. Due to the non-isotropic distribution of the emitted photons, the photon yield as detected by the two detectors at the upstream and downstream end of the electron lens is slightly different. However, the functional dependence on beam offset and crossing angle is very similar.

This dependency of the photon rate on the detector is to be compared with the effect of a simultaneous shift of both beams while colliding head-on. Shifting both beams with respect to the photon detector changes the number of detected photons, as shown in Figure 4. Since this rate change is negligible compared to the effect of a relative offset of the two beams by the same amount, this demonstrates that a single photon detector at each end of the overlap section is sufficient.

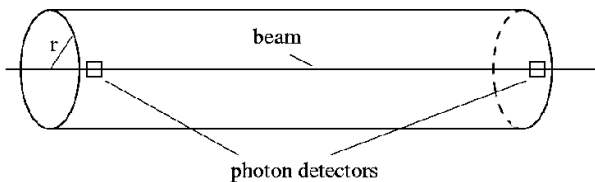


Figure 3: Photon detector configuration

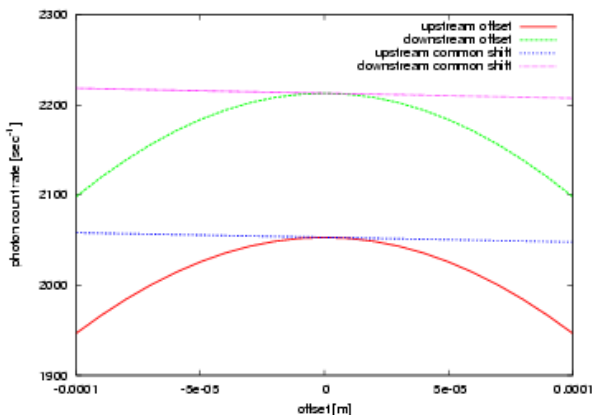


Figure 4: Photon rate as function of relative beam-beam offset  $\Delta r$  at the upstream (red) and downstream (green) photon detectors. The blue and magenta lines show the photon rate at the two detectors as function of a common shift of the electron and proton beam.

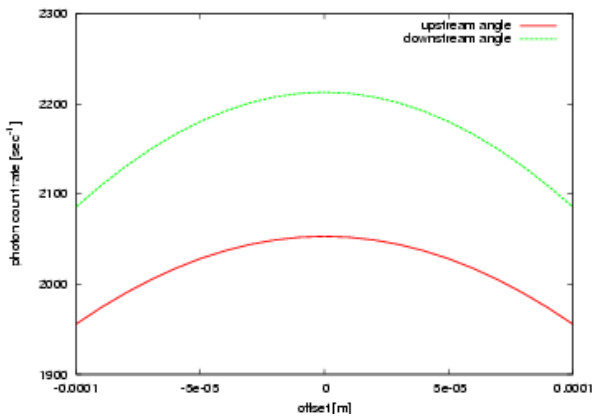


Figure 5: Photon rate as function of crossing angle  $\phi$  at the two photon detectors.

### BACKGROUND CONSIDERATIONS

Several sources of background may contaminate the collision signal picked up by the photon detectors. Collisions of the beam with residual gas molecules cause excitation and ionization of the residual gas, which may lead to photon emission. However, the associated cross section for photon production [4] is several orders of magnitude smaller than the ionization cross section [5].

Large-angle elastic scattering events occur during the collision of the proton and electron beams, leading to electrons spiraling around the magnetic field lines of the electron lens solenoid. The spiraling electrons will therefore emit synchrotron radiation that may hit the photon detector.

These background sources result in photon energies in the IR to UV spectrum. To improve the signal-to-noise ratio in the photon detector, shielding the detector from low-energy photons below a few keV by means of a thin metallic coating is therefore under consideration.

In this case, the detector consists of a YAP:Ce scintillator crystal [6] that converts the energy deposited by the high energy bremsstrahlung photons into visible photons at a conversion rate of 20 photons/keV. Given a total photon energy of approximately 75 MeV/second deposited in the crystal, a secondary photon rate of 1.5 million photons per second is produced. These visible photons will be transported by a dedicated optical system to either a microchannel plate or a photomultiplier.

If the background from low-energy photons is small enough compared to the bremsstrahlung photon count rate in the visible spectrum, these visible bremsstrahlung photons could be detected directly, using a microchannel plate or a photomultiplier.

### ACKNOWLEDGMENTS

The authors would like to thank W. Nakel and A. Pikin for numerous valuable discussions.

### REFERENCES

- [1] W. Fischer et al., "Status of the RHIC head-on beam-beam compensation project", these proceedings
- [2] E. Haug, W. Nakel, "The elementary process of bremsstrahlung", World Scientific lecture notes in physics 73
- [3] J. D. Jackson, Classical Electrodynamics, 2nd ed., Wiley, New York, 1975
- [4] T. Tsang et al., Rev. Sci. Instrum. 79, 105103 (2008)
- [5] A. G. Mathewson, O. Gröbner, Thermal Outgassing and Beam Induced Desorption, in: A. Chao, M. Tigner (eds.), Handbook of Accelerator Physics and Engineering, World Scientific
- [6] M. Moszyński et al., Nucl. Instr. Meth. A 404 (1998) 157 - 165